

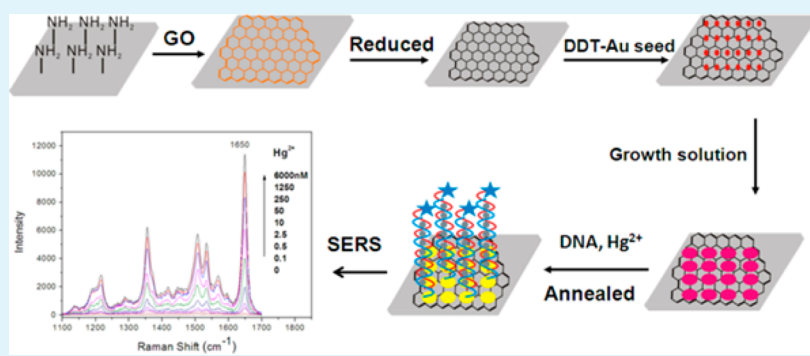
Highly Sensitive SERS Detection of Hg^{2+} Ions in Aqueous Media Using Gold Nanoparticles/Graphene Heterojunctions

Xiaofeng Ding,^{†,‡} Lingtao Kong,^{*,†} Jin Wang,[†] Fang Fang,[†] Dandan Li,[†] and Jinhuai Liu^{*,†}

[†]Research Center for Biomimetic Functional Materials and Sensing Devices, Institute of Intelligent Machines, Chinese Academy of Sciences, Hefei, Anhui 230031, China

[‡]School of Life Science, Anhui University, Hefei, Anhui 230039, China

Supporting Information



ABSTRACT: Gold nanoparticles (AuNPs)/reduced graphene oxide (rGO) heterojunctions were synthesized directly on SiO_2/Si substrates via a seed-assisted growth process. The in situ chemical fabrication strategy has been proven to be quite simple and efficient for generating highly active surface-enhanced Raman scattering (SERS) substrates due to synergistic enhanced protocol from rGO and AuNPs. The SERS substrates with AuNPs/rGO heterojunctions have been utilized for trace analysis of mercury(II) ions via thymine– Hg^{2+} –thymine coordination. Thereby, very low limits of detection, i.e., 0.1 nM or 20 ppt for Hg^{2+} , can be achieved in contrast with some other SERS substrates, which suggests that the heterojunctions are appropriate as versatile surface-enhanced substrates applied in chemical sensing or biosensing.

KEYWORDS: reduced graphene oxide, gold nanoparticles, heterojunctions, SERS, sensor

1. INTRODUCTION

Heavy-metal contaminations have been becoming one of the most challenging problems in the 21st century. In particular, the mercury(II) (Hg^{2+}) ion is generally considered to be one of the most toxic pollutants in that it has severe effects on not only the production environment but also human health.^{1–7} Accordingly, it is important to develop a selective and sensitive method for the detection of Hg^{2+} ions. Up to now, numerous traditional detection methods, e.g., biosensor,⁸ resonance scattering,⁹ ELISA,¹⁰ atomic absorption spectroscopy,¹¹ fluorescence,¹² and colorimetric,¹³ have been used to detect Hg^{2+} ions. In contrast, surface-enhanced Raman scattering (SERS), as one of the most sensitive detection technologies, has received wide recognition in many industries^{14–17} because of its high sensitivity, noninvasiveness, fluorescence-quenching properties, high resolution, and fingerprint information about the chemical structures. Recently, Chung et al. have reported SERS detection of Hg^{2+} ions by using a single gold microshell.¹⁸ Kim et al. employed a gold-nanowire-on-film SERS sensor to obtain ultrasensitive Hg^{2+} detection.¹⁹ Therefore, it is necessary to develop novel sensitive and selective SERS substrates for detecting Hg^{2+} .

At present, graphene is being widely applied in many fields, such as lithium-ion batteries,²⁰ supercapacitors,²¹ photovoltaic devices,²² photocatalysis,²³ and electrochemistry,²⁴ because of its exceptional properties. However, a recent investigation revealed that graphene possesses SERS properties so as to be used as a SERS substrate.²⁵ Hence, it can be anticipated that graphene as a SERS substrate will bring a new opportunity for developing SERS technology. As far as the present graphene/noble metallic nanoparticle composites^{26,27} are concerned, gold nanoparticles (AuNPs) are often mainly attached to graphene through layer-by-layer assembly, which somewhat affects their stabilities or binding degrees as SERS substrates. However, if AuNPs/graphene composites are obtained by an in situ growth approach, it can be expected to improve the binding strength and contribute to the promotion of free electron mobility for yielding heterojunctions between AuNPs and graphene. More importantly, the formation of heterojunctions in the composites^{28–30} has led to many unique electronic, optical,

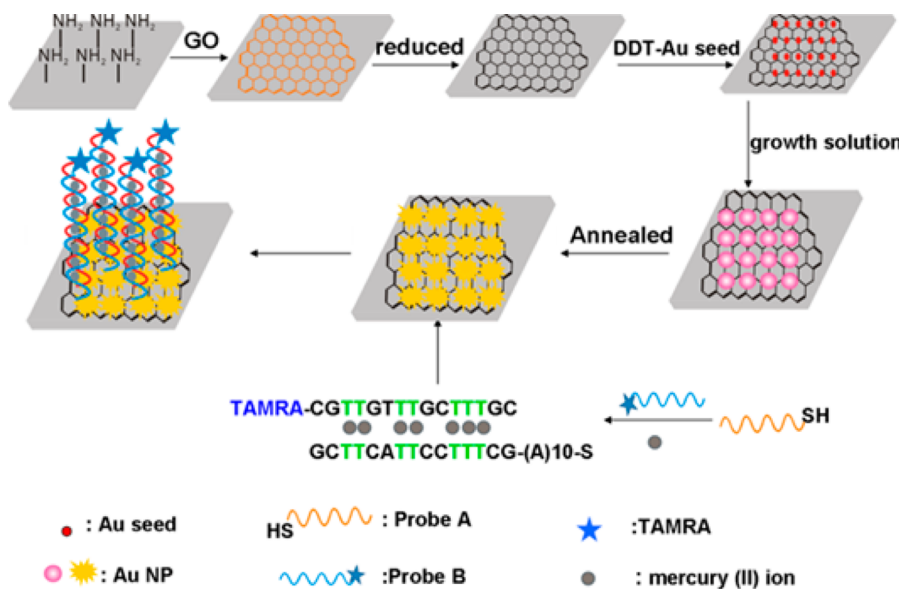
Received: April 15, 2013

Accepted: July 15, 2013

Published: July 15, 2013



Scheme 1. Schematic Illustration of the Fabrication of AuNPs/rGO Heterojunction SERS Active Substrates and a Sensing Protocol for Hg^{2+} Ions



and magnetic properties for applications in nanoelectronics, optoelectronics, plasmonics, medical diagnostics, catalysis, drug delivery, therapeutics, separations, chemical sensing, etc.

Herein, on the basis of seed-assisted growth methods, we have developed high-performance AuNPs/graphene heterojunction SERS active substrates via AuNP *in situ* direct growth onto the surface of reduced graphene oxide (rGO) substrates, which shows strong local surface plasmon resonance (LSPR) absorption strength and highly sensitive SERS enhancement effects. After modification of DNA with specific sequences, it can be used for the detection of heavy-metal contaminations, displaying ultrasensitivity and selectivity, e.g., mercury-specific oligonucleotide, in that the formation of thymine– Hg^{2+} complexes has been well established; moreover, some novel Hg^{2+} nanobiosensing assay protocols based on a thymine– Hg^{2+} –thymine (T– Hg^{2+} –T) mismatch are being developed.^{31,32}

2. EXPERIMENTAL SECTION

2.1. Materials. Natural graphite, 3-N-morpholinopropanesulfonic acid (MOPS), and (3-aminopropyl)triethoxysilane (APTES) were obtained from Aldrich. KMnO_4 , NaNO_3 , H_2SO_4 (98%), H_2O_2 (30%), HAuCl_4 , 1-dodecanethiol (DDT), NaBH_4 , AgNO_3 , ascorbic acid (AA), hexadecyltrimethylammonium bromide (CTAB), crystal violet (CV), and ethanol were all analytical grade and were purchased from Shanghai Chemical Co. Ltd. DNA oligonucleotides were synthesized and purified by Sangon (Shanghai, China) and used without further purification. Water was purified using a Millipore filtration system (Milli-Q water). All aqueous solutions were prepared with ultrapure water (>18 MU).

2.2. Fabrication of AuNPs/rGO Heterojunctions and a SERS Sensing Protocol for Hg^{2+} . The *in situ* direct growth of AuNPs on the surface of a rGO substrate is described as follows in detail. The fabrication of AuNPs/rGO heterojunctions and a SERS sensing protocol for Hg^{2+} are shown in the following schematic graph (Scheme 1).

2.3. Preparation of rGO/SiO₂/Si Substrates. The 300-nm SiO₂/Si substrate was cleaned in a piranha solution (3:1 ratio of 98% H_2SO_4 and 30% H_2O_2 ; **caution!** piranha solution is a strong oxidant and should not be mixed with organic solvents) for 1 h, followed by rinsing with deionized water and ethanol, and drying with a nitrogen gas stream. A NH₂-terminated self-assembled monolayer (SAM) substrate was prepared by immersing the piranha-treated substrate in a 5% (v/v)

APTES solution in ethanol for 1 h,³³ sonicating in toluene for 2 min, washing with water and ethanol, and drying under a stream of nitrogen. The substrate was annealed at 105 °C for 1 h to stabilize the APTES SAM layer. Then, the substrate was immersed in the graphene oxide (GO) prepared by a modified Hummer's method³⁴ (see the detailed synthesis procedure in the Supporting Information), suspended (8000 rpm for 10 min) for 1 h, washed with water and ethanol, and dried under a stream of nitrogen. Finally, the substrate was thermally annealed at 180 °C for 10 min to induce amide bonding between APTES and GO film.^{35,36} The rGO film substrate is achieved by reducing the GO substrate in a hydrazine vapor environment (shown in Scheme 1).

2.4. Preparation of AuNPs/rGO Heterojunctions on SiO₂/Si Substrates. First, the averaged 1.5-nm-diameter gold seed solution prepared with 5 mL of 200 mM CTAB, 5 mL of 0.5 mM HAuCl₄, and 0.6 mL of 10 mM NaBH₄ was extracted by 2 mL of DDT. Then, the rGO/SiO₂/Si substrate was immersed in the DDT-modified seed solution for about 2 h, washed with ethanol, and dried under a stream of nitrogen. Finally, the seed-modified rGO/SiO₂/Si substrate was immersed in an aqueous growing solution containing 5 mL of 200 mM CTAB, 5 mL of 1 mM HAuCl₄, and 0.05 mL of AA for 2 h at 28 °C. After rinsing with water and drying with a gentle flow of nitrogen, the as-prepared AuNPs/rGO/SiO₂/Si substrate was annealed at 500 °C in an ultrapure N₂ atmosphere to obtain an AuNPs/rGO heterojunction SERS substrate (shown in Scheme 1).

2.5. Hg²⁺ Detection by Using SERS on the AuNPs/rGO/SiO₂/Si Substrates. First, 100 μL of thiolated capture DNA1 (1 μM), 20 μL of different concentrations of Hg^{2+} , and 100 μL of DNA2 (1 μM) labeled with tetramethylrhodamine (TAMRA) were mixed in a MOPS buffer solution (10 mM MOPS with 50 mM NaNO₃, pH 7.2) and shaken for over 20 min. Then, the substrate was immersed in this solution for 10 min, followed by rinsing with a MOPS buffer solution to remove the unbound capture DNAs. The substrate was rinsed with water and dried with nitrogen and then used for SERS detection (shown in Scheme 1).

2.6. Instrumentation. The morphology of graphene was examined by atomic force microscopy (AFM; MultiMode V, Veeco, USA). Scanning electron microscopy (SEM; QUANTA 200FEG, America), optical microscopy, and UV-vis-near-IR (NIR; SOLID 3700, Japan) were used to observe rGO and the nanoheterojunctions based on AuNPs directly grown on the rGO surface in SiO₂/Si or glass substrates. SERS analysis was performed by using a HR800 Raman microscope instrument (Horiba, Jobin Yvon, France) with a standard 532 nm He/Ne 10 mW laser with a laser spot size of 1 μm . X-ray

photoelectron spectrometry (XPS) was carried out on an ESCALab MK II by using non-monochromatized Mg Ka X-ray beams as the excitation source. Binding energies were calibrated relative to the C 1s peak at 284.6 eV.

3. RESULTS AND DISCUSSION

GO was synthesized by a modified Hummer's method and demonstrated with SEM, UV-vis-NIR, Raman spectroscopy, and XPS analysis (see Figures 1s–4s in the Supporting Information). AuNPs/rGO heterojunctions were synthesized directly on SiO₂/Si substrates by the four steps shown in Scheme 1 (see the Experimental Section for full details). Briefly, GO sheets are first adsorbed to APTES-modified SiO₂/Si substrates through NH₂ groups. After reduction in a hydrazine vapor environment, rGO/SiO₂/Si substrates can be obtained. Subsequently, DDT monolayer-protected gold seeds (MPSs) of 1.5 nm diameter are adsorbed to the rGO/SiO₂/Si substrates through hydrophobic interactions. After that, AuNPs can be in situ grown on rGO/SiO₂/Si through a seed-assisted process. Finally, high-temperature annealing in an ultrapure N₂ atmosphere can enhance the intimate contacts between AuNPs and rGO so as to move the impurities for obtaining AuNPs/rGO heterojunctions. In order to prove the mechanical and thermal stability of the rGO/SiO₂/Si substrate, the SEM images of the substrates before and after these treatments, such as immersed in the DDT-modified seed solution, immersed in the aqueous growing solution, and annealed at 500 °C in an ultrapure N₂ atmosphere, are given in the Supporting Information (see Figure 5s). From these SEM images, it can be found that the rGO films and AuNP morphologies could still efficiently remain on the surface of the SiO₂/Si substrates after many steps of treatment.

As shown in Figure 1A,B, the AFM image of rGO shows that the thickness of the synthesized rGO is less than 1 nm, indicating that exfoliated monolayer rGO sheets can be adsorbed onto an amine-functionalized SiO₂/Si substrate by electrostatic interactions and a subsequent thermal treatment can increase the stability of the rGO thin films. Previous investigations suggested that the thickness and uniformity of

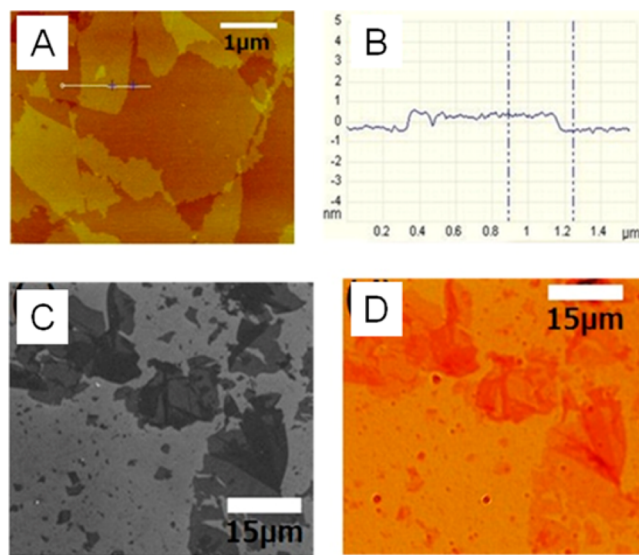


Figure 1. (A) AFM image of rGO. (B) Section analysis of part A. (C) SEM image of rGO membranes on SiO₂/Si substrates. (D) Optical image of identical rGO films on SiO₂/Si substrates.

the rGO films on SiO₂/Si substrates could also be evaluated via color contrast.^{37,38} Hence, identical regions of rGO on SiO₂/Si substrates in SEM experiments have been chosen for optical microscopic observations, which indicate that the thickness of rGO is 1–2 layers of graphene, which is shown in Figure 1C,D.

Adsorption of gold seeds on rGO/SiO₂/Si substrates can be ascribed to hydrophobic interactions between the dodecyl chain in DDT and the surface of rGO, and these seeds provide large quantities of sites for subsequent growth. Thereby, AuNPs are grown directly onto the functionalized rGO substrates through a seed-assisted growth process. Both the SEM and optical images reveal that the AuNPs with diameter of 70–80 nm can be densely and uniformly grown on the rGO/SiO₂/Si substrates (see Figure 2), which is very significant for the formation of highly active heterojunction SERS substrates.

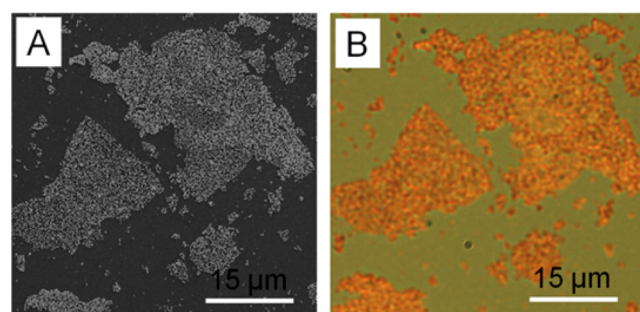


Figure 2. (A) SEM image of the AuNPs/rGO heterojunction based on AuNPs grown on the surface of rGO-coated substrates via the seed-mediated approach. (B) Optical image of the heterojunctions in the same area on the substrate.

To study the LSPR characteristics of AuNPs/rGO, SiO₂/Si substrates have to be replaced by glass chips so as to remove interference of silicon in the visible regions. In Figure 3, plots a

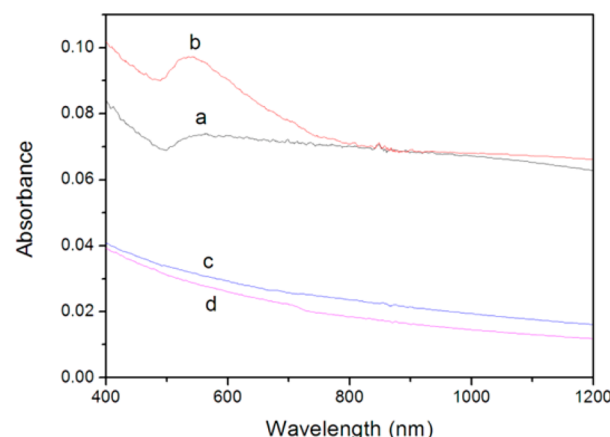


Figure 3. UV-vis-NIR spectra of (a) the AuNPs/rGO heterojunction, (b) the AuNPs/rGO heterojunction annealed at 500 °C in an ultrapure N₂ atmosphere, (c) MPSs/APTES/glass, and (d) rGO/APTES/glass placed in a growth solution.

and b are UV-vis-NIR spectra of AuNPs/rGO heterojunctions on glass substrates before and after annealing at 500 °C in an ultrapure N₂ atmosphere, respectively. The absorbance intensity of the LSPR band at 539 nm in curve a is obviously 1.3 times higher than that in curve b, suggesting that the annealing treatment can efficiently strengthen the

interaction between AuNPs and rGO. In contrast, no LSPR characteristics are exhibited in curve c (MPSs/APTES/glass) and curve d (rGO/APTES/glass), indicating that adsorption of AuNPs on the MPSs/APTES/glass surface or rGO/APTES/glass is quite weak. Hence, an *in situ* seed-assisted process combined with an annealing treatment has been proven to be an efficient pathway for generating AuNPs/rGO heterojunctions. Moreover, it can be expected that the present heterojunctions are appropriate as SERS active substrates because of SERS effect dependence on the LSPR characteristics of AuNPs.

Raman spectroscopy is commonly used to characterize rGO,³⁹ and AuNPs are known to enhance Raman scattering signals.⁴⁰ Figure 4 shows the G and D bands respectively of the

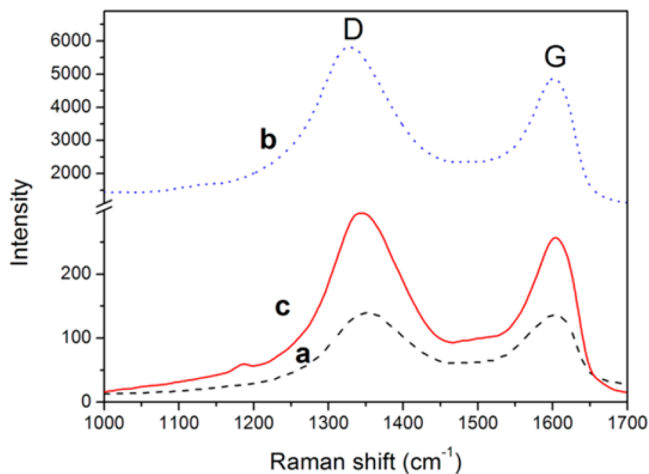


Figure 4. Raman spectra depicting G and D bands of rGO/ SiO_2/Si (a) and AuNPs/rGO/ SiO_2/Si heterojunction substrates before (b) and after annealing (c).

spectra of rGO/ SiO_2/Si (plot a) and AuNPs/rGO/ SiO_2/Si before (plot b) and after (plot c) annealing at 500 °C in an ultrapure N₂ atmosphere. The presence of AuNPs enhanced the SERS signals 40-fold in comparison with blank substrates, implying that generation of a heterojunction can remarkably increase the Raman signals. Interestingly, the Raman signals dramatically decrease to 3-fold enhancement compared to blank substrates after an annealing treatment, which could be ascribed to a dense gold coating on the surface of rGO.

In control experiments, the other three substrates (SiO_2/Si , rGO/ SiO_2/Si , and AuNPs/ SiO_2/Si) were designed to prove whether the AuNPs/rGO/ SiO_2/Si heterojunction substrate can be used as an effective SERS substrate. Their Raman spectra were measured after a droplet of a CV dye (1 μM) solution, which usually is used as a probe for the evaluation of a SERS substrate, was dropcasted onto the surface of these substrates. As shown in Figure 5A, the Raman signals of CV on the AuNPs/rGO/ SiO_2/Si heterojunction substrate are the strongest in the four substrates. As is well-known, SERS enhancement typically comes from two mechanisms, namely, a chemical mechanism (CM) and an electromagnetic mechanism (EM).^{41,42} A recent investigation suggested that graphene can be used as a SERS substrate because of the CM, i.e., charge transfer between the Raman probe molecules and graphene.²⁵ On the other hand, the EM effect is mainly ascribed to a large increase of the local electric field caused by LSPR of nanoscale metals, such as silver nanoparticles and AuNPs.⁴³ In the present

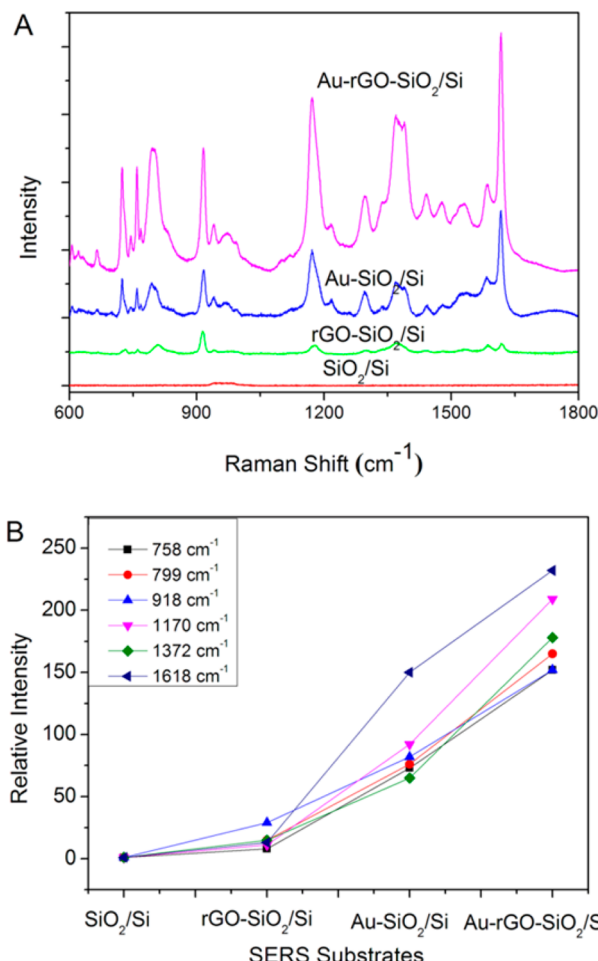


Figure 5. (A) Raman spectra of 1 μM CV on SiO_2/Si , rGO/ SiO_2/Si , AuNPs/ SiO_2/Si , and AuNPs/rGO/ SiO_2/Si heterojunction substrates. (B) Relative Raman intensities of six fingerprint Raman peaks of CV on different substrates, compared with the intensities of CV on the bare SiO_2/Si substrate.

case, we believe that the two mechanisms can simultaneously contribute to the overall enhancement. According to the relative Raman intensity analysis from six fingerprint Raman peaks of CV (758, 799, 918, 1170, 1372, and 1618 cm^{-1}) on these different substrates, the relative intensities of the six peaks of CV on rGO/ SiO_2/Si substrate are 8, 15, 29, 11, 15, and 13, the relative intensities of the six peaks of CV on AuNPs/ SiO_2/Si substrate are 73, 76, 82, 92, 65, and 150, and the relative intensities of the six peaks of CV on AuNPs/rGO/ SiO_2/Si substrate are 152, 165, 152, 209, 178, and 232 (shown in Figure 5B). Therefore, SERS signals on the AuNPs/ SiO_2/Si substrate are much stronger than those on the rGO/ SiO_2/Si substrate but are weaker than those on the AuNPs/rGO/ SiO_2/Si heterojunction substrate. For further verification of whether the SERS enhancement results from annealing, the CV SERS spectra on AuNPs/ SiO_2/Si substrates before and after annealing at 500 °C were measured and compared, as shown in the Supporting Information (see Figure 6s). It can be found that their Raman intensities are almost the same. All of these results support that the enhancement is from both AuNPs and graphene because of the dramatic synergistic enhancement from AuNPs and rGO in the heterojunctions.

In order to test the uniformity of the AuNPs/rGO/ SiO_2/Si heterojunction SERS substrates, we collected the SERS spectra

of CV by a 2D point mapping mode. As shown in Figure 6, a $17 \times 18 \mu\text{m}$ area of the AuNPs/rGO/SiO₂/Si heterojunction

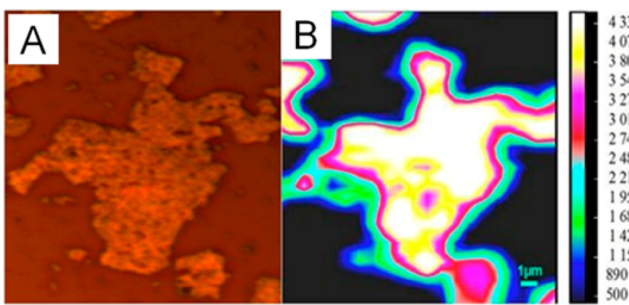


Figure 6. (A) Optical image of the area for the AuNPs/rGO/SiO₂/Si heterojunction SERS substrate. (B) 2D SERS mapping of the substrate following CV adsorption. The peak mapped was 1618 cm^{-1} . Laser wavelength: 532 nm. Power: 10 mW. Lens: 50× objective. Acquisition time: 2 s.

substrate was chosen. The peak at 1618 cm^{-1} could be mapped, and the strong SERS signals at each point demonstrated that the substrate has good reproducibility. The value of the relative standard deviation of the band at 1618 cm^{-1} is 12.8%. The results indicate that the AuNPs/rGO/SiO₂/Si heterojunction substrate is an excellent SERS active substrate with high quality.

Having established that the AuNPs/rGO heterojunction is a SERS active substrate, we employed it for Hg²⁺ detection by immobilizing thiolated DNA on AuNPs. The detection protocol can be described as chelation of Hg²⁺ in a thymine–thymine mismatch via T-Hg²⁺-T⁴⁴ on DNA-functionalized AuNPs.^{12,18,45}

In the present case, we utilized two noncomplementary probes (probe A, SH-A₁₀-GCT TTG CTT ACT TCG; probe B, TAMRA-CGT TGT TTG CTT TGC). As mentioned in the experimental details, using DNA, probe A can be immobilized on the AuNPs/rGO/SiO₂/Si heterojunction substrates by strong interaction between SH and Au, and the SERS-labeled TAMRA-tagged probe B can be bound to the heterojunction substrates via T-Hg²⁺-T. In order to evaluate the sensitivity of SERS detection, different concentrations of Hg²⁺ ranging from 0.1 to 6000 nM can be analyzed through the AuNPs/rGO/SiO₂/Si heterojunction SERS active substrates. As shown in Figure 7A, strong SERS signals from TAMRA-labeled DNA can be observed at 1650, 1533, 1508, 1355, and 1217 cm^{-1} ⁴⁶ only when Hg²⁺ was added, and the SERS intensity is weakened, accompanied by the descent of the concentration of Hg²⁺. The SERS intensity of the vibrational band at 1650 cm^{-1} , which is quite highly sensitive to the concentration of Hg²⁺, suggests that the present limits of detection can be as low as the 0.1 nM (0.02 ppb) level according to the 3σ rule (where σ is the standard deviation of a blank solution and $n = 5$), which, to the best of our knowledge, is the lowest in SERS detection of the Hg²⁺ ion in contrast with some other SERS substrates. It is worth pointing out that the physical adsorption of dye molecules on AuNPs is relatively weak;⁴⁷ however, the shorter length of the DNA strand compared to the size of AuNPs can efficiently improve the absorption efficiency of dye molecules on DNA-conjugated AuNPs. Particularly, dye molecules can be surrounded by a dense AuNP layer of the AuNPs/rGO/SiO₂/Si heterojunction substrates.

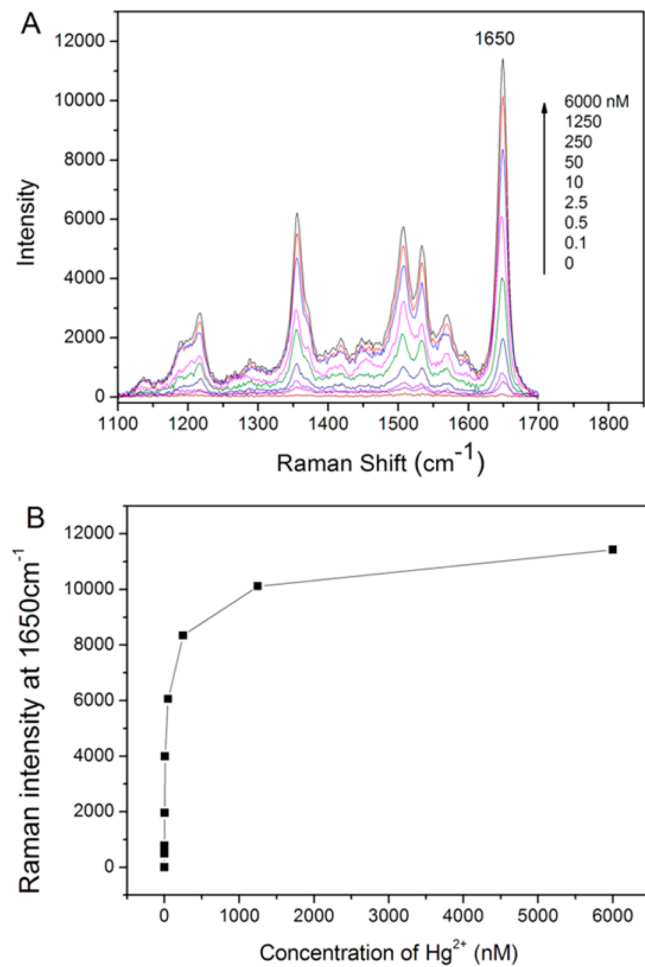


Figure 7. (A) SERS spectra obtained at a variety of Hg²⁺ ion concentrations from 0.1 to 6000 nM. (B) Plot demonstration of how the Raman intensity at 1650 cm^{-1} changes upon the addition of different concentrations of Hg²⁺ ions.

The selectivity of the substrate was determined in the presence of various competing divalent metal or alkaline ions such as Mg²⁺, Cu²⁺, K⁺, Ni²⁺, Mn²⁺, Zn²⁺, Na⁺, Co²⁺, Cd²⁺, and Pb²⁺ at a concentration of 1 μM (Figure 8). Remarkably, no

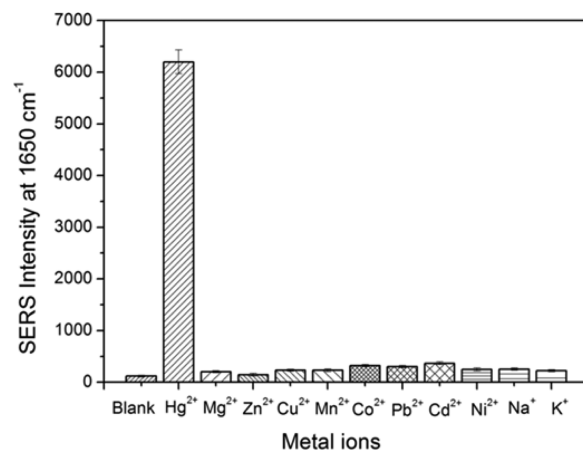


Figure 8. Selectivity of the present AuNPs/rGO/SiO₂/Si heterojunction SERS active substrate detection on the other metal ions (1 μM) compared to Hg²⁺ (50 nM).

apparent SERS signal changes of the substrate are observed with these metal ions, even at high concentrations; only Hg²⁺ results in a significant increase in the SERS signal. These results clearly demonstrate that the SERS substrate functionalized with a mercury-specific oligonucleotide is highly selective toward Hg²⁺ over the other metal ions. The specific selective detection for Hg²⁺ ions is attributed mainly to be formation of stable T-Hg²⁺-T complexes thanks to chelation of Hg²⁺ in a thymine–thymine mismatch via T-Hg²⁺-T on DNA-functionalized AuNPs in the heterojunction SERS substrates.

4. CONCLUSIONS

In summary, we have developed AuNPs/rGO/SiO₂/Si heterojunction SERS active substrates through AuNP *in situ* direct growth onto the surface of rGO. The AuNPs/rGO/SiO₂/Si substrate exhibits high SERS activity because of the synergistic enhancement of AuNPs and rGO in the heterojunctions. It is interesting that after an annealing treatment the heterojunction SERS substrates can show much stronger LSPR absorption intensity, i.e., 1.3 times higher than that of the unannealed substrate. The excellent SERS performance of the heterojunctions should be relevant to their LSPR characteristics. Moreover, the heterojunctions can act as excellent SERS platforms for the trace detection of Hg²⁺ ions, which display ultrasensitivity (0.1 nM or 20 ppt) and high selectivity. Compared to some other mercury(II) sensors, the heterojunction SERS sensor exhibits 500 times stronger responses.⁴⁸ Thus, we expect that AuNPs/rGO/SiO₂/Si heterojunction SERS active substrates can offer a new opportunity for small volume analysis of not only Hg²⁺ ions but also some other toxic metal ions in environmental and biological samples.

■ ASSOCIATED CONTENT

Supporting Information

Synthesis and characterization of GO, SEM images of the rGO/SiO₂/Si substrates after different treatments, and CV Raman spectra on the AuNPs/SiO₂/Si substrate before and after 500 °C annealing. This material is available free of charge via the Internet at <http://pubs.acs.org>.

■ AUTHOR INFORMATION

Corresponding Author

*E-mail: ltkong@iim.ac.cn (L.K.), jhliu@iim.ac.cn (J.L.). Tel: +86-551-65591142. Fax: +86-551-65592420.

Notes

The authors declare no competing financial interest.

■ ACKNOWLEDGMENTS

This work was supported by the National Natural Science Foundation of China (Grants 21177131 and 21077106), the National Key Scientific Program-Nanoscience and Nanotechnology (Grant 2011CB933700), and a China Postdoctoral Science Foundation funded project (Grant 20110490834).

■ REFERENCES

- Campbell, L. M.; Dixon, D. G.; Hecky, R. E. *J. Toxicol. Environ. Health, Part B* **2003**, *6*, 325–356.
- Schneider, L.; Peleja, R. P.; Kluczkoński, A., Jr.; Freire, G. M.; Marioni, B.; Vogt, R. C.; Silveira, R. D. *Arch. Environ. Contam. Toxicol.* **2012**, *63*, 270–279.
- Reardon, A. M.; Bhat, H. K. *Toxicol. Environ. Chem.* **2007**, *89*, 535–554.
- Wang, Y.; Bolland, M. E.; Nicholson, J. K.; Holmes, E. J. *Pharm. Biomed. Anal.* **2006**, *40*, 375–381.
- Virtanen, J. K.; Rissanen, T. H.; Voutilainen, S.; Tuomainen, T. P. *J. Nutr. Biochem.* **2007**, *18*, 75–85.
- da Silva, D. A. F.; Barbosa, F.; Scarano, W. R. *J. Exp. Path.* **2012**, *93*, 354–360.
- Grandjean, P.; Weihe, P.; White, R. F.; Debes, F.; Araki, S.; Yokoyama, K.; Murata, K.; Sørensen, N.; Dahl, R.; Jørgensen, P. J. *Neurotoxicol. Teratol.* **1997**, *19*, 417–428.
- Lee, C.; Choo, J. *Bull. Korean Chem. Soc.* **2011**, *32*, 2003–2007.
- Wu, Y.; Zhan, S.; Xu, L.; Shi, W.; Xi, T.; Zhan, X.; Zhou, P. *Chem. Commun.* **2011**, *47*, 6027–6029.
- Zhang, Y.; Li, X.; Liu, G.; Wang, Z.; Kong, T.; Tang, J.; Zhang, P.; Yang, W.; Li, D. N.; Liu, L.; Xie, G.; Wang, J. *Biol. Trace Elem. Res.* **2011**, *144*, 854–864.
- Shah, A. Q.; Kazi, T. G.; Baig, J. A.; Afridi, H. I.; Arain, M. B. *Food Chem.* **2012**, *134*, 2345–2349.
- Ye, B. C.; Yin, B. C. *Angew. Chem., Int. Ed.* **2008**, *47*, 8386–8389.
- Lou, T.; Chen, L.; Zhang, C.; Kang, Q.; You, H.; Shen, D.; Chen, L. *Anal. Methods* **2012**, *4*, 488–491.
- Lu, F.; Zhang, S.; Gao, H.; Jia, H.; Zheng, L. *ACS Appl. Mater. Interfaces* **2012**, *4*, 3278–3284.
- Cerf, A.; Molnár, G.; Vieu, C. *ACS Appl. Mater. Interfaces* **2009**, *11*, 2544–2550.
- Li, X.; Hu, H.; Li, D.; Shen, Z.; Xiong, Q.; Li, S.; Fan, H. J. *ACS Appl. Mater. Interfaces* **2012**, *4*, 2180–2185.
- Li, J.; Chen, L.; Lou, T.; Wang, Y. *ACS Appl. Mater. Interfaces* **2011**, *3*, 3936–3941.
- Han, D.; Lim, S. Y.; Kim, B. J.; Piao, L.; Chung, T. D. *Chem. Commun.* **2010**, *46*, 5587–5589.
- Kang, T.; Yoo, S. M.; Yoon, I.; Lee, S.; Choo, J.; Lee, S. Y.; Kim, B. *Chem.—Eur. J.* **2011**, *17*, 2211–2214.
- Arico, A. S.; Bruce, P.; Scrosati, B.; Tarascon, J.-M.; Schalkwijk, W. V. *Nat. Mater.* **2005**, *4*, 366–377.
- Liu, C.; Li, F.; Ma, L.-P.; Cheng, H.-M. *Adv. Mater.* **2010**, *22*, E28–E62.
- Sun, S. R.; Gao, L.; Liu, Y. Q. *Appl. Phys. Lett.* **2010**, *96*, 083113.
- Williams, G.; Seger, B.; Kamat, P. V. *ACS Nano* **2008**, *2*, 1487–1491.
- Shan, C.; Yang, H.; Song, J.; Han, D.; Ivaska, A.; Niu, L. *Anal. Chem.* **2009**, *81*, 2378–2382.
- Ling, X.; Xie, L.; Fang, Y.; Xu, H.; Zhang, H.; Kong, J.; Dresselhaus, M. S.; Zhang, J.; Liu, Z. *Nano Lett.* **2010**, *10*, 553–561.
- Liu, J.; Li, Y.; Li, Y.; Li, J.; Deng, Z. *J. Mater. Chem.* **2010**, *20*, 900–906.
- Liu, J.; Fu, S.; Yuan, B.; Li, Y.; Deng, Z. *J. Am. Chem. Soc.* **2010**, *132*, 7279–7281.
- Xiong, Y.; Mayers, B. T.; Xia, Y. *Chem. Commun.* **2005**, 5013–5022.
- Wang, F.; Dong, A.; Sun, J.; Tang, R.; Yu, H.; Buhro, W. E. *Inorg. Chem.* **2006**, *45*, 7511–7521.
- Hurst, S. J.; Payne, E. K.; Qin, L.; Mirkin, C. A. *Angew. Chem., Int. Ed.* **2006**, *45*, 2672–2692.
- He, S. J.; Li, D.; Zhu, C. F.; Song, S. P.; Wang, L. H.; Long, Y. T.; Fan, C. H. *Chem. Commun.* **2008**, *40*, 4885–4887.
- Liu, C. W.; Hsieh, Y. T.; Huang, C. C.; Lin, Z. H.; Chang, H. T. *Chem. Commun.* **2008**, *19*, 2242–2244.
- Sarveswaran, K.; Hu, W. C.; Huber, P. W.; Bernstein, G. H.; Lieberman, M. *Langmuir* **2006**, *22*, 11279–11283.
- Hummers, W. S.; Offeman, R. E. *J. Am. Chem. Soc.* **1958**, *80*, 1339.
- Yun, J. M.; Kim, K. N.; Kim, J. Y.; Shin, D. O.; Lee, W. J.; Lee, S. H.; Lieberman, M.; Kim, S. O. *Angew. Chem., Int. Ed.* **2011**, *50*, 1–5.
- Kim, Y.-K.; Na, H.-K.; Lee, Y. W.; Jang, H.; Min, S. W. H.-H. *Chem. Commun.* **2010**, *46*, 3185–3187.
- Kim, Y.-K.; Na, H.-K.; Min, D.-H. *Langmuir* **2010**, *26*, 13065–13070.

- (38) Luo, Z.; Lu, Y.; Somers, L. A.; Johnson, A. T. C. *J. Am. Chem. Soc.* **2009**, *131*, 898–899.
- (39) Kong, L. T.; Wang, J.; Zheng, G.; Liu, J. H. *Chem. Commun.* **2011**, *47*, 10389–10391.
- (40) Wang, J.; Kong, L. T.; Guo, Z.; Xu, J. Y.; Liu, J. H. *J. Mater. Chem.* **2010**, *20*, 5271–5279.
- (41) Adrian, F. J. *J. Chem. Phys.* **1982**, *77*, 5302–5314.
- (42) King, F. W.; Van Duyne, R. P.; Schatz, G. C. *J. Chem. Phys.* **1978**, *69*, 4474–4481.
- (43) Moskovits, M. *Rev. Mod. Phys.* **1985**, *57*, 783–826.
- (44) Miyake, Y.; Togashi, H.; Tashiro, M.; Yamaguchi, H.; Oda, S.; Kudo, M.; Tanaka, Y.; Kondo, Y.; Sawa, R.; Fujimoto, T.; Machinami, T.; Ono, A. *J. Am. Chem. Soc.* **2006**, *128*, 2172–2173.
- (45) Ren, W.; Zhu, C.; Wang, E. *Nanoscale* **2012**, *4*, 5902–5909.
- (46) Faulds, K.; Fruk, L.; Robson, D. C.; Thompson, D. G.; Enright, A.; Smith, W. E.; Graham, D. *Faraday Discuss.* **2006**, *132*, 261–268.
- (47) Lu, G.; Li, H.; Liusman, C.; Yin, Z. Y.; Wu, S. X.; Zhang, H. *Chem. Sci.* **2011**, *2*, 1817–1821.
- (48) Bera, R. K.; Das, A. K.; Raj, C. R. *Chem. Mater.* **2010**, *22*, 4505–4511.